Two-mass DOB Robust to Elastic Coefficient Variation for Collaborative Robot Joint Using Joint Torque Sensor and Encoders

Akiyuki Hasegawa* Student Member, Hiroshi Fujimoto* Senior Member
Taro Takahashi** Member

A collaborative robot is a robot that can work with humans in a shared workspace. Collaborative robots can improve productivity and compensate for the shortage of working population. To make safe contact with a human, backdrivability is necessary. For high backdrivability, a robot with a joint torque sensor or a load-side encoder has been developed. We previously proposed a filtered disturbance observer for a high backdrivable robot joint using motor-side and load-side encoders. In the method, we used the nominal elastic coefficient parameter to calculate joint torque. However, the elastic coefficient of robot joint fluctuates depending on the torsion angle. In other words, a control method which is robust to the elastic coefficient variation is adequate for joint control. In this paper, we apply the filtered DOB method to the two-mass system using encoders and torque sensor. Our proposed method is robust to elastic coefficient variation.

The performance of the proposed method is validated by simulation and experiment.

Keywords: collaborative robot, two-mass, disturbance suppression, load-side encoder, torque sensor, torque control, backdrivability

1. Introduction

In recent years, collaborative robots gather attention. A collaborative robot is a robot that can work with humans in a shared workspace. It is expected that they can improve productivity and compensate for the shortage of working population in industry and the field of welfare [1]. There is a big difference between a collaborative robot and a conventional robot. A collaborative robot should have the ability to contact safe with a human. To make safe contact with a human, backdrivability is necessary for robot joint. In other words, for a collaborative robot, not only position control but also backdrivability is required to realize a safe contact [2].

A collaborative robot is often equipped with a 6 DOF sensor on end effector to measure contact force. However, in this way, we cannot measure contact force on any part except end effector. We can solve this problem by measuring joint torque, because contact force effect can be estimate from joint torque information. Therefore, it is reasonable to measure and control joint torque, instead of the contact force. To measure joint torque or torsion angle, robots incorporating a torque sensor or a load-side encoder in their each joint have been developed [3] [4] [5]. In addition, Torobo Arm of Tokyo Robotics [6], Panda of Franka Emika [7], Sawyer of Rethink Robotics [8], etc. are beginning to be sold as torque controllable robots.

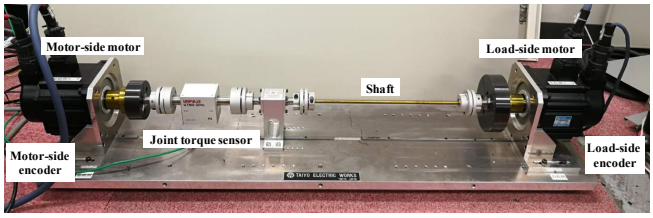

Fig. 1: Experimental machine of a two-mass motor bench

Not only hardware but also control theory is developed, for realizing a collaborative robot. Torque control method for a multiple joints robot is studied [9]. Research on bilateral control, which requires coordination of position control and force control, is studied [10] [11]. We previously proposed the filtered DOB for high backdrivable two-mass system [12]. In the method, we applied the filtered DOB to a robot joint with motor-side and load-side encoders. To measure the joint torque, we calculated from torsion angle and the nominal elastic coefficient value. However, the elastic coefficient value often fluctuates depending on torsion angle. Therefore the control method which is robust to the elastic coefficient variation is adequate for robot joint control.

In this paper, we apply the filtered DOB method to the two-mass system using encoders and torque sensor. Our proposed method is robust to elastic coefficient variation.

2. Experimental Setup and Modeling

Fig. 1 shows the experimental machine of a two-mass motor bench. The experimental machine has not only the motor-

* The University of Tokyo
5-1-5, Kashiwanoha, Kashiwa, Chiba, 227-8561 Japan
Phone: +81-4-7136-3881
Email: akiyuki.hasegawa@ieee.org
** Mobile Manipulator Robot Group, 2020 Robot Development Dept., T-Frontier Div., Frontier Research Center, Toyota Motor Corporation
543, Kirigahora, Nishihirose-cho, Toyota, Aichi, 470-0309 Japan
Phone: +81-566-98-6468
Email: taro_takahashi@mail.toyota.co.jp

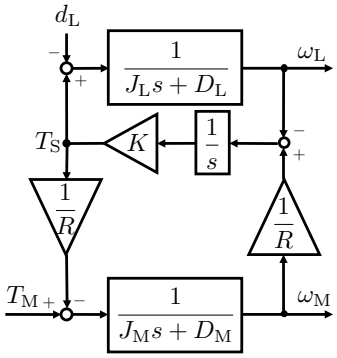

Fig. 2: Block diagram of two-mass system

side encoder but also the load-side one. In addition, it has a joint torque sensor. Therefore, it is possible to implement a control method using information about the load-side angle and joint torque.

In this paper, taking elastic bodies into account, each joint is modeled as a two-mass system which is shown in Fig. 2. The frequency characteristic from the input torque to the motor-side angle is shown in Fig. 3. and one from the input torque to the load-side angle is shown in Fig. 4. The solid black line indicates measured data, the broken blue line indicates the two-mass model.

Table. 1 shows the modeling parameters of the motor bench. Frequency domain signal design method [13] was used for system identification. At the time of measurement.

The equation of motion for the two-mass system is indicated by (1) and (2). The joint torque T_S caused by the elasticity of the gear. In our proposed method, we consider that the joint torque changes linearly to the angular difference as shown in (3).

$$\left(J_\mathrm{M}s^2 + D_\mathrm{M}s\right)\theta_\mathrm{M} = T_\mathrm{M} - \frac{1}{R}T_\mathrm{S} \tag{1}$$

$$\left(J_\mathrm{L}s^2 + D_\mathrm{L}s\right)\theta_\mathrm{L} = T_\mathrm{S} - d_\mathrm{L} \tag{2}$$

$$T_\mathrm{S} = K\left(\frac{1}{R}\theta_\mathrm{M} - \theta_\mathrm{L}\right) \tag{3}$$

From these equations, the respective transfer functions are obtained as follows.

$$G_{\theta_\mathrm{M}T_\mathrm{M}} = \frac{J_\mathrm{L}s^2 + D_\mathrm{L}s + K}{D(s)} \tag{4}$$

$$G_{\theta_\mathrm{L}T_\mathrm{M}} = \frac{1}{R}\frac{K}{D(s)} \tag{5}$$

$$G_{\theta_\mathrm{M}d_\mathrm{L}} = -\frac{1}{R}\frac{K}{D(s)} \tag{6}$$

$$G_{\theta_\mathrm{L}d_\mathrm{L}} = -\frac{J_\mathrm{M}s^2 + D_\mathrm{M}s + \frac{K}{R^2}}{D(s)} \tag{7}$$

$$D(s) = J_\mathrm{M}J_\mathrm{L}s^4 + (J_\mathrm{L}D_\mathrm{M} + J_\mathrm{M}D_\mathrm{L})\,s^3$$

Table 1: Parameters of the motor bench

J_M	Motor-side moment of inertia	0.0020 N ms^2/rad
J_L	Load-side moment of inertia	0.0057 N ms^2/rad
D_M	Motor-side viscosity friction coefficient	0.006 N ms/rad
D_L	Load-side viscosity friction coefficient	0.0859 N ms/rad
K	Torsional rigidity coefficient	93.6137 N m/rad
R	Gear ratio	1

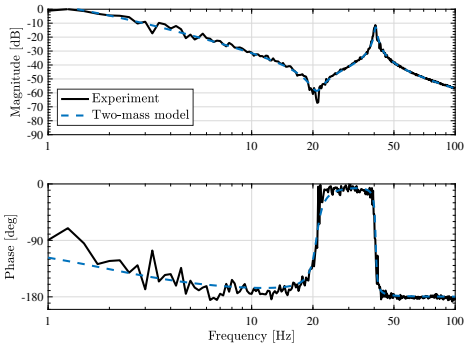

Fig. 3: From the motor input torque T_M to the motor-side angle θ_M.

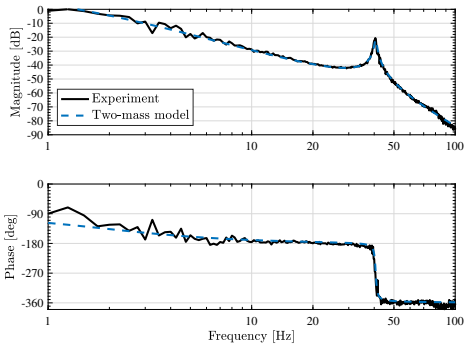

Fig. 4: From the motor input torque T_M to the load-side angle θ_L.

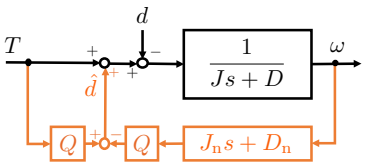

Fig. 5: Block diagram of DOB for one-mass system

$$+\left(KJ_\mathrm{M} + \frac{K}{R^2}J_\mathrm{L} + D_\mathrm{M}D_\mathrm{L}\right)s^2$$
$$+\left(KD_\mathrm{M} + \frac{K}{R^2}D_\mathrm{L}\right)s \tag{8}$$

G_{AB} indicates the transfer function from B to A.

3. Disturbance Observer

3.1 DOB for one-mass system Disturbance Observer (DOB) is widely used to eliminate the influence of input disturbance. It is a kind of simplified state observer. Fig. 5 shows a block diagram of DOB for a one-mass system.

T denotes input torque, d denotes input disturbance torque. The equation of motion for a one-mass plant is indicated by (9).

$$(Js + D)\,\omega = T - d \tag{9}$$

DOB estimates the disturbance torque using this equation. The estimation of the input disturbance by DOB is expressed by (10).

$$\hat{d} = [T - (J_\mathrm{n}s + D_\mathrm{n})\,\omega]\,Q(s) \tag{10}$$

$Q(s)$ is a parameter of DOB. Generally, a low-pass filter is used as a Q-filter. The gain of $Q(s)$ at low frequencies should be 1 for compensating the influence of stationary disturbance, and gain at high frequency should be almost 0 for reducing the influence of high-frequency noise. In addition to that, $(Js + D)\,Q(s)$ should be proper.

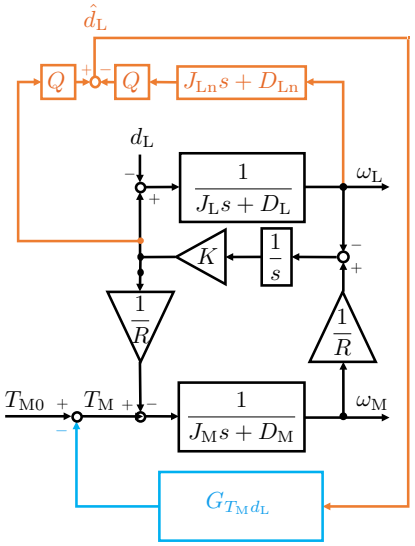

Fig. 6: Block diagram of the system with Filtered DOB

For a one-mass system, the influence of disturbance is eliminated easily with the estimation and the simple feedback system.

3.2 Problem in DOB for two-mass system For a two-mass system, it is difficult to eliminate the influence of load-side disturbance by simple DOB. The estimation of d_L is possible with the simple observer. Estimation of the load-side disturbance by DOB is expressed by (11).

$$\hat{d}_\mathrm{L} = [T_\mathrm{S} - (J_\mathrm{Ln}s + D_\mathrm{Ln})\,\omega_\mathrm{L}]\,Q(s) \qquad (11)$$

However, if the estimated load-side disturbance is inputted to the motor side, the influence cannot be compensated. Theoretical problems are described below using analysis by comparison of transfer functions.

When the load-side disturbance d_L is added, θ_L changes by the amount of $G_{\theta_\mathrm{L} d_\mathrm{L}} d_\mathrm{L}$. In order to eliminate this influence, d_L should be estimated firstly. Let $\hat{d}_\mathrm{L}$ be an estimated value of d_L. If $\hat{d}_\mathrm{L}$ is added to input torque T_M, θ_L changes by the amount of $G_{\theta_\mathrm{L} T_\mathrm{M}} \hat{d}_\mathrm{L}$.

However, $G_{\theta_\mathrm{L} T_\mathrm{M}}$ and $G_{\theta_\mathrm{L} d_\mathrm{L}}$ are very different. Therefore, $G_{\theta_\mathrm{L} T_\mathrm{M}} \hat{d}_\mathrm{L}$ cannot cancel out $G_{\theta_\mathrm{L} d_\mathrm{L}} d_\mathrm{L}$ effectively,

3.3 DOB for two-mass system using torsion angle (Conventional method) Sehoon *et al.* proposed joint torque control method using DOB for Series Elastic Actuator (SEA) [14]. SEA is modeled as a two-mass system. Therefore, the DOB can be applied to robot joint using electric motor actuators. Fig. 8 shows the block diagram of the joint torque control method using the DOB. We call it a torsion angle DOB in this paper. Their proposed method also use a feedforward controller, however we focus on only DOB to compare the performance of DOBs. Torsional angle DOB is also disappears the effect on the joint torque from load-side disturbance.

3.4 DOB filter for joint torque control (proposed method) We showed that the influence of load-side disturbance to a two-mass system cannot be compensated by a simple DOB theoretically.

However, if we chose a physical output value that the influence of load-side disturbance should be eliminated, there are cases that the influence only on the output values can be eliminated with DOB and an appropriate filter.

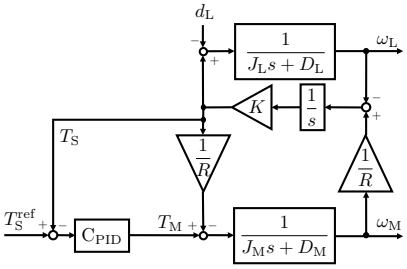

Fig. 7: Block diagram of PID control for Joint torque without DOB (Conventional Method 1)

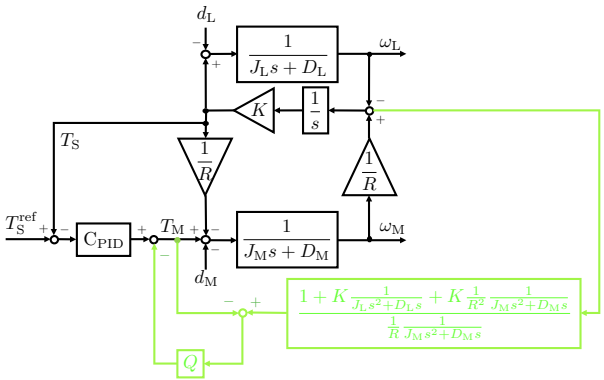

Fig. 8: Block diagram of PID control for Joint torque with Filtered DOB (Conventinal Method 2)

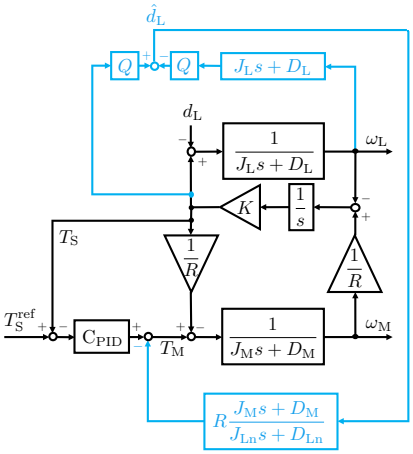

Fig. 9: Block diagram of the system with Filtered DOB (Proposed method)

In this paper, we chose the joint torque as an output value, because it is one of the important values for implementing collaborative robots. When the influence of disturbance to the joint torque is eliminated, the joint is not twisted by the disturbance force, therefore the joint gets high backdrivability. Design of the appropriate filter for joint-torque control is expressed below. Fig. 6 shows the system in the form of a block diagram. $G_{T_\mathrm{S} T_\mathrm{M}}$ indicates the transfer function from motor-side torque T_M to joint torque T_S and $G_{T_\mathrm{S} d_\mathrm{L}}$ indicates one from load-side torque d_L to joint torque T_S. $G_{T_\mathrm{S} T_\mathrm{M}}$ and $G_{T_\mathrm{S} d_\mathrm{L}}$ are denoted in (12) and (13), respectively.

$$\begin{aligned} G_{T_\mathrm{S} T_\mathrm{M}} &= \frac{K}{R} G_{\theta_\mathrm{M} T_\mathrm{M}} - K G_{\theta_\mathrm{L} T_\mathrm{M}} \\ &= \frac{K}{R} \frac{J_\mathrm{L}s^2 + D_\mathrm{L}s}{D(s)} \end{aligned} \qquad (12)$$

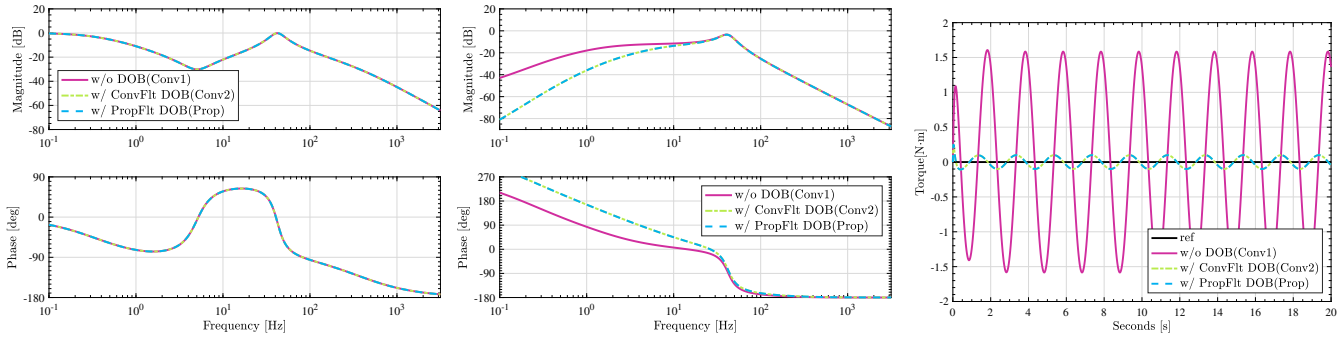

(a) Frequency response from the joint torque reference $T_{\mathrm{S}}^{\mathrm{ref}}$ to the joint torque T_{S}

(b) Frequency response from the load-side disturbance d_{L} to the joint torque T_{S}

(c) Time response of the joint torque T_{S}

Fig. 10: Simulaton results ($K_{\mathrm{n}} = K$)

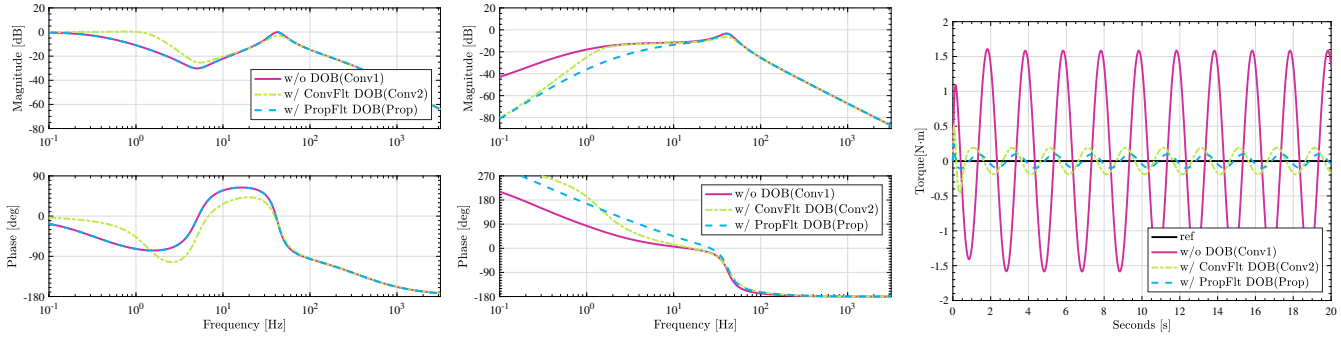

(a) Frequency response from the joint torque reference $T_{\mathrm{S}}^{\mathrm{ref}}$ to the joint torque T_{S}

(b) Frequency response from the load-side disturbance d_{L} to the joint torque T_{S}

(c) Time response of the joint torque T_{S}

Fig. 11: Simulaton results ($K_{\mathrm{n}} = 0.2K$)

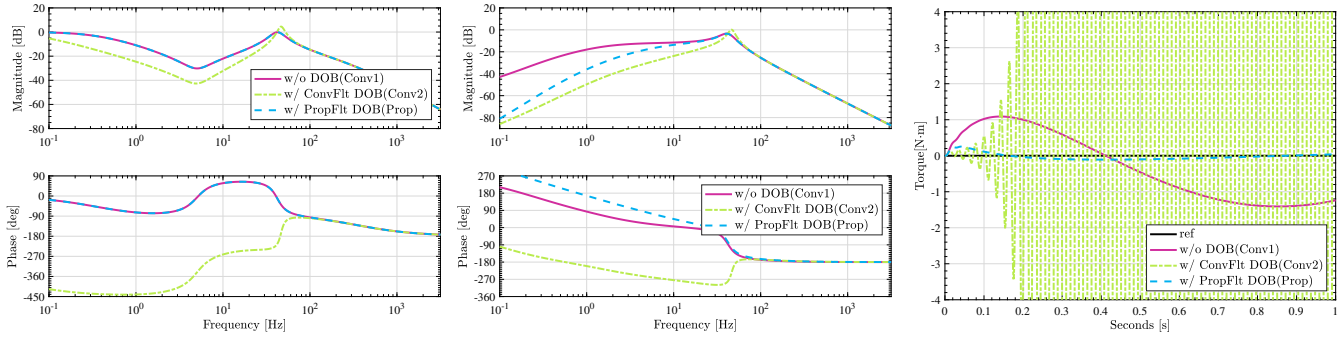

(a) Frequency response from the joint torque reference $T_{\mathrm{S}}^{\mathrm{ref}}$ to the joint torque T_{S}

(b) Frequency response from the load-side disturbance d_{L} to the joint torque T_{S}

(c) Time response of the joint torque T_{S}

Fig. 12: Simulaton results ($K_{\mathrm{n}} = 5K$)

$$G_{T_{\mathrm{S}}d_{\mathrm{L}}} = \frac{K}{R} G_{\theta_{\mathrm{M}}d_{\mathrm{L}}} - K G_{\theta_{\mathrm{L}}d_{\mathrm{L}}} = K \frac{J_{\mathrm{M}} s^2 + D_{\mathrm{M}} s}{D(s)} \tag{13}$$

Joint torque considering multiple inputs on the motor side and the load side is denoted by (14).

$$T_{\mathrm{S}} = G_{T_{\mathrm{S}}T_{\mathrm{M}}} T_{\mathrm{M}} + G_{T_{\mathrm{S}}d_{\mathrm{L}}} d_{\mathrm{L}} \tag{14}$$

We defined $G_{T_{\mathrm{M}}d_{\mathrm{L}}}$ as the transfer function of the appropriate filter. When the load-side disturbance is added and $\hat{d}_{\mathrm{L}}$ is added to the input signal through the filter as shown in Fig. 6, the joint torque T_{S} is represented by (15).

$$T_{\mathrm{S}} = G_{T_{\mathrm{S}}T_{\mathrm{M}}} \left(T_{\mathrm{M0}} - G_{T_{\mathrm{M}}d_{\mathrm{L}}} \hat{d}_{\mathrm{L}} \right) + G_{T_{\mathrm{S}}d_{\mathrm{L}}} d_{\mathrm{L}} = G_{T_{\mathrm{S}}T_{\mathrm{M}}} T_{\mathrm{M0}} - G_{T_{\mathrm{S}}T_{\mathrm{M}}} G_{T_{\mathrm{M}}d_{\mathrm{L}}} \hat{d}_{\mathrm{L}} + G_{T_{\mathrm{S}}d_{\mathrm{L}}} d_{\mathrm{L}} \tag{15}$$

T_{M0} is the original input torque value.

It can be said that disturbance compensation is successful, if the terms of d_{L} and $\hat{d}_{\mathrm{L}}$ cancel each other. When the disturbance estimation is normally performed, $d_{\mathrm{L}} = \hat{d}_{\mathrm{L}}$ is established, therefore (16) is obtained from the terms of d_{L} and $\hat{d}_{\mathrm{L}}$ in (15).

$$\left(G_{T_{\mathrm{S}}T_{\mathrm{M}}} G_{T_{\mathrm{M}}d_{\mathrm{L}}} + G_{T_{\mathrm{S}}d_{\mathrm{L}}} \right) d_{\mathrm{L}} \simeq 0 \tag{16}$$

Transfer function of the filter indicated by (17) is obtained by transforming (16)

$$G_{T_{\mathrm{M}}d_{\mathrm{L}}} = G_{T_{\mathrm{S}}T_{\mathrm{M}}}^{-1} G_{T_{\mathrm{S}}d_{\mathrm{L}}} = \frac{RD(s)}{K(J_{\mathrm{L}} s^2 + D_{\mathrm{L}} s)} \frac{K(J_{\mathrm{M}} s^2 + D_{\mathrm{M}} s)}{D(s)}$$

$$= R\frac{J_M s + D_M}{J_L s + D_L} \tag{17}$$

Thus, the filter for compensating the influence on the joint torque from the load-side disturbance was obtained.

When $\hat{d}_L = d_L Q(s)$ is established considering the influence of the Q-filter, (18) is obtained by calculating the terms of d_L and $\hat{d}_L$ in (15).

$$\begin{aligned} T_S &= G_{T_S T_M} T_{M0} + G_{T_S d_L} d_L - G_{T_S T_M} G_{T_M d_L} \hat{d}_L \\ &= G_{T_S T_M} T_{M0} + \frac{K(J_M s^2 + D_M s)}{D(s)} d_L \\ &\quad - \frac{K}{R}\frac{J_L s^2 + D_L s}{D(s)} R \frac{J_M s + D_M}{J_L s + D_L} d_L Q(s) \\ &= G_{T_S T_M} T_{M0} + \frac{K(J_M s^2 + D_M s)}{D(s)} (1 - Q(s))\, d_L \end{aligned} \tag{18}$$

It is understood that when $Q(s) = 1$, the influence on the joint torque from the load-side disturbance completely disappears.

As a result, the transfer function from d_L to θ_L is expressed by (19).

$$G_{\theta_L d_L} = \frac{1}{J_L s^2 + D_L s} \tag{19}$$

(19) shows that the influence of elastic body and motor side to the backdrivability disappears, the backdrivability is improved.

4. Simulation

Simulations evaluated the performance of each methods.

The conventional method 1 is PID control without DOB as shown in Fig. 7, the conventional method 2 is PID control with joint torque DOB as shown in Fig. 8, and the proposed method is PID control with filtered DOB as shown in Fig. 9. Every PID controllers is same, the time constant of DOB is 0.02 s.

4.1 K is coincide with nominal value K_n Fig. 10a shows the frequency response from the joint torque reference T_S^{ref} to the joint torque T_S. Since the PID controllers of the three methods have the same gain , the frequency characteristics are also the same.

Fig. 10b shows the frequency response from the load-side disturbance torque d_L to the joint torque T_S. In the proposed method and the conventional method 2, the gain became smaller, the effect of the disturbance is greatly suppressed. When the nominal value coincide the real value, the proposed method and the conventional method 2 has the same performance.

Fig. 10c shows the time response of the joint torque. 1 Hz Sine wave load-side disturbance is added. The conventional method 2 and the proposed method has the same good performance as with the frequency response.

4.2 K is not coincide with nominal value K_n Next, we showed the other simulation results. In the simulation, the elastic coefficient value K is not coincide with nominal value.

In Fig. 11, the nominal value of the elastic coefficient K_n is 0.2 times as large as the true value K. Fig. 11a shows the frequency response from the joint torque reference T_S^{ref} to the joint torque T_S. Fig. 11b shows the frequency response from the load-side disturbance torque d_L to the joint torque T_S.

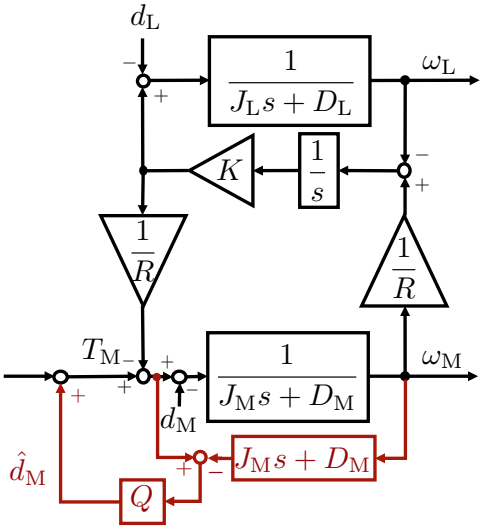

Fig. 13: The block diagram of motor-side disturbance observer

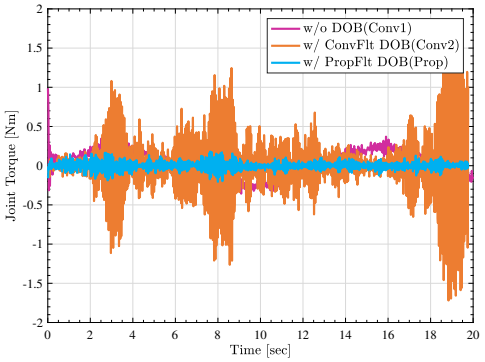

Fig. 14: Time response of joint torque ($K = 5K_n$)

Regarding the conventional method 2, the control bandwidth becomes higher. On the other hand, the disturbance suppression performance is degraded. In the results, the reference following performance of the conventional method is lower than that of the proposed method as shown in Fig. 11c.

In Fig. 12, the nominal value of the elastic coefficient K_n is 5 times as large as the true value K. Fig. 11a shows the frequency response from the joint torque reference T_S^{ref} to the joint torque T_S. Fig. 11b shows the frequency response from the load-side disturbance torque d_L to the joint torque T_S. Regarding the conventional method 2, the disturbance suppression performance is better. On the other hand, the control bandwidth is declined. In the results, time response is unstable as shown in Fig. 11c.

Basically, the torsion angle DOB and proposed method has higher performance. When the nominal elastic coefficient doesn't coincide with real value, the performance of the torsional angle DOB is changed. On the other hand, proposed method is robust to the elastic coefficient variation. It is because that the torsion angle DOB need parameter K, however our proposed method doesn't use the K.

The elastic coefficient of harmonic drive depend on the torsion angle, so the DOB should robust to the elastic coefficient variation. From this perspective, our proposed method is better than the conventional methods.

5. Experiment

In the experiments, the joint torque 0 Nm control was conducted. Unlike simulation, the two-mass plant has friction disturbance. Conventional method 2 DOB suppresses the motor-side disturbance. In this experiment, we want compare the load-side disturbance suppression performance. Therefore, the motor-side disturbance observer is added to the conventional method 1 and the proposed method as shown in Fig. 13.

Fig. 14 shows the exprimental result of the joint torque time response. The load-side disturbance torque is 1 Hz sine wave. The nominal value of the elastic coefficient K_{n} is 5 times as large as the true value K. Conventional method 2 become unstable, because the performance of the method is affected the variation of the elastic coefficient value. Proposed method doesn't need the elastic coefficient value for the controller parameters. Therefore we can design the joint torque controller robust to the variation of the elastic coefficient value.

6. Conclusion

Development of a collaborative robot equipped with joint torque sensors or load-side encoders is expanding. To realize a safe contact by using sensor information, the effective control method is needed. In this paper, we proposed the method which makes backdrivability higher by DOB robust to the elastic coefficient variation. By considering the structure of a two-mass system and designing the DOB filter, we greatly improved the backdrivability of two-mass system. The performance is evaluated by simulations and experiments.

References

(1) TOYOTA, "Partner Robot." [Online]. Available: https://www.toyota-global.com/innovation/partner_robot/robot

(2) N. Motoi and R. Kubo, "Human-Machine Cooperative Grasping / Manipulating System Using Force-based Compliance Controller with Force Threshold," *IEEJ Journal of Industry Applications*, vol. 5, no. 2, pp. 39–46, 2015.

(3) C. Semini, V. Barasuol, J. Goldsmith, M. Frigerio, M. Focchi, Y. Gao, S. Member, and D. G. C. Member, "Design of the Hydraulically-Actuated , Torque-Controlled Quadruped Robot HyQ2Max," *IEEE/ASME Transactions on Mechatronics*, no. 99, pp. 1–12, 2016.

(4) J. Vorndamme, M. Schappler, A. Tödtheide, and S. Haddadin, "Soft robotics for the hydraulic Atlas arms: Joint impedance control with collision detection and disturbance compensation," *IEEE International Conference on Intelligent Robots and Systems*, vol. 2016-Novem, pp. 3360–3367, 2016.

(5) C. Schindlbeck and S. Haddadin, "Unified passivity-based Cartesian force/impedance control for rigid and flexible joint robots via task-energy tanks," *Proceedings - IEEE International Conference on Robotics and Automation*, vol. 2015-June, no. June, pp. 440–447, 2015.

(6) TokyoRobotics, "Torobo Arm." [Online]. Available: http://robotics.tokyo/products/torobo_arm/

(7) FrankaEmika, "Panda." [Online]. Available: https://www.franka.de/

(8) RethinkRobotics, "High performance collaborative robot." [Online]. Available: https://www.rethinkrobotics.com/sawyer/

(9) F. Petit and A. Dietrich, "Generalizing Torque Control Concepts to Variable Stiffness Robots," *IEEE Robotics and Automation Magazine*, vol. 22, no. 4, pp. 37–51, 2015.

(10) J. Kim, P. H. Chang, and H. S. Park, "Two-channel transparency-optimized control architectures in bilateral teleoperation with time delay," *IEEE Transactions on Control Systems Technology*, vol. 21, no. 1, pp. 40–51, 2013.

(11) H. Sakai and D. Tomizuka, "Compliance Control for Stabilization of Bilateral Teleoperation System in the Presence of Time Delay," in *IEEE International Conference on Mechatronics*, 2017.

(12) A. Hasegawa, H. Fujimoto, and T. Takahashi, "Filtered Disturbance Observer for High Backdrivable Robot Joint," in *The 44th Annual Conference of the IEEE Industrial Electronics Society*, Washington D.C., USA, 2018, pp. 5086–5091.

(13) J. Pitelon, Rik Schoukens, *System Identification: A Frequency Domain Approach, 2nd Editon*. Wiley-IEEE Press, 2012.

(14) S. Oh and K. Kong, "High-Precision Robust Force Control of a Series Elastic Actuator," *Transactions on Mechatronics*, vol. 22, no. 1, pp. 71–80, 2017.